

Article

Characterization of Two Main Forest Cover Loss Transitions in North Korea from 1990 to 2020

Yihua Jin ¹, Jingrong Zhu ¹, Guishan Cui ², Zhenhao Yin ^{2,*}, Weihong Zhu ^{2,*} and Dong Kun Lee ³¹ College of Agriculture, Yanbian University, Yanji 133002, China; jinyh2018@ybu.edu.cn (Y.J.)² College of Geography and Ocean Science, Yanbian University, Yanji 133002, China³ Department of Landscape Architecture and Rural System Engineering, Seoul National University, Seoul 151-743, Republic of Korea; dkleee7@snu.ac.kr

* Correspondence: yzh2015@ybu.edu.cn (Z.Y.); whzhu@ybu.edu.cn (W.Z.); Tel.: +86-130-4338-0770 (Z.Y.)

Abstract: This study aims to characterize forest cover transitions in North Korea and identify deforested areas that are degraded or at risk of degradation. We used phenological information and random forest classifiers to perform a deforestation classification. We then extracted the two main forest cover loss patterns, sloping farmland (farmland with slope greater than 6 degrees) and unstocked forest (crown cover less than 20%), for the years of 2000, 2010, and 2020. Based on the deforestation map of each year, we analyzed the deforestation dynamics from 1990 to 2020. Forests showed decreases in cover by 27% over the 30-year study period and accounted for 41.5% of the total land area in 2020. Deforestation spread into the core area, which led to severe shrinkage and fragmentation of forests. Unstocked forest and sloping farmland experienced the highest rates of loss among the forestland uses and accounted for 48.9% and 39.3% of the total loss over the study period, respectively. During the study period, 25,128 km², 5346 km², and 6728 km² of forestland was cleared, degraded, and was at risk of degradation or barrenness by artificial repeated fires, respectively. This methodological framework provides a valuable template for areas that are difficult to access, and the deforestation dynamics results can provide a basis for conservation and sustainable management of forest resources.

Keywords: deforestation; forest degradation; reforestation; sloping farmland; unstocked forest; random forest classifier; MOD13Q1



Citation: Jin, Y.; Zhu, J.; Cui, G.; Yin, Z.; Zhu, W.; Lee, D.K. Characterization of Two Main Forest Cover Loss Transitions in North Korea from 1990 to 2020. *Forests* **2023**, *14*, 1966. <https://doi.org/10.3390/f14101966>

Academic Editors: Filiz Bektas Balcik, Fusun Balik Sanli, Fabiana Caló and Antonio Pepe

Received: 7 August 2023

Revised: 24 September 2023

Accepted: 26 September 2023

Published: 28 September 2023



Copyright: © 2023 by the authors. Licensee MDPI, Basel, Switzerland. This article is an open access article distributed under the terms and conditions of the Creative Commons Attribution (CC BY) license (<https://creativecommons.org/licenses/by/4.0/>).

1. Introduction

Deforestation has become an important issue in terms of climate change mitigation and ecosystem services, and its main adverse effects are increased aridity, biodiversity decline, climate change, and erosion damage [1]. With the growing demand for agricultural expansion and development in developing countries, deforestation has become the greatest threat to sustainable development, especially in mountainous areas and developing countries [2,3]. Moreover, repeated deforestation and forest land use, along with abandonment, negatively affect the environment and lead to extreme forest degradation [4].

In North Korea, deforestation is a major threat to current and future ecological security. Ecosystem services from forests in North Korea have decreased dramatically due to severe deforestation [5]. Unstocked forests and sloping farmland are the two main types of forest cover loss transitions. Sloping farmland in North Korea is defined as forest with slopes greater than 6 degrees that have been transformed into farmland to produce crops, while unstocked forest is defined as forest that has been denuded or presents crown cover less than 20% caused by logging or artificial forest fires [6]. The two main transitions are caused by recurring man-made fire disturbances, crop production, and fuel logging. Large areas of sloping farmland are observed when large tracts of forestland are converted to farmland. Moreover, continuous cultivation and lack of sustainable farming practices lead to a decline in soil fertility and productivity and a subsequent loss of vegetation cover. Instead of

implementing sustainable farming techniques or land regeneration, farmers often choose to abandon degraded plots and cultivate new areas, and by repeating this process they ignore the ecological capacity of the land to recover. As a result, sloping farmland in North Korea that was created by sacrificing forest ecosystems is unsustainable. Furthermore, soils in once-forested areas have lost their ecological function and resilience, resulting in widely distributed denuded slopes [7].

Due to its mountainous terrain, North Korea is already highly vulnerable to natural disasters, and its depleted forests show exacerbated soil erosion and poor water retention. These factors have significantly increased the risk of extreme weather events, such as flash floods and landslides [8,9]. Deforestation has played a major role in the environmental degradation of North Korea. The combination of natural disasters, extreme weather events, and deforestation, and the resulting soil loss have created an unsustainable environment. In addition, North Korea is an important location in the ecological network of Northeast Asia and plays a vital connecting role on the Korean Peninsula. To systematically prioritize restoration and planning efforts, the regional forestland use characteristics and spatial and temporal deforestation changes must be better understood [10].

Deforestation has been a major global concern due to its significant impact on biodiversity, climate change, and ecosystem services [11]. Remote-sensing (RS) techniques have emerged as valuable tools for monitoring and characterizing deforestation patterns at various scales. Several remote-sensing-based techniques have been explored to map and monitor deforestation. These include supervised and unsupervised classification methods [12], object-based image analysis (OBIA) [13], and machine learning algorithms [14,15]. These approaches utilize spectral, spatial, and textural information to identify deforestation patterns, distinguish forest cover types, and detect changes over time. Additionally, the use of Synthetic Aperture Radar (SAR) data has shown promising results in overcoming limitations related to cloud cover and illumination conditions [16,17]. Beyond deforestation detection, RS techniques have contributed to assessing forest degradation. This includes the estimation of canopy cover loss [18], biomass reduction [19], and fragmentation analysis using RS-derived metrics [20]. Through the integration of RS with field data and ground-based measurements, researchers have been able to quantify the ecological impacts of deforestation and highlight areas at high risk of degradation.

Remote-sensing technology has revolutionized the field of environmental monitoring, particularly in land use and deforestation analysis. However, when it comes to North Korea, remote-sensing-based classification of land use or deforestation encounters specific limitations due to limited ground truth information. Previous studies have explored the use of remote-sensing techniques to map land use in North Korea. This involves analyzing satellite imagery to classify and identify different land cover types [21,22], such as forests, agricultural lands, urban areas, and water bodies [23]. Researchers have utilized time-series remote-sensing data to detect and monitor land use changes in North Korea. By comparing multiple images acquired over different time periods, identify areas where land cover has transformed, providing insights into patterns of urbanization, deforestation [24], and agricultural expansion [25]. However, they only examining forest area dynamics did not account for the different categories of forest cover, low level types.

Confusing data on vegetation cover types represent a major problem when working with single remotely sensed datasets in North Korea. Thus, limitations arise because a single image can only provide limited information and may not capture the full complexity and variability of vegetation types. In addition, different vegetation types may have similar spectral responses, which increase the difficulty of accurately classifying such vegetation based on a single image. Additionally, classification accuracy may be affected by various factors, such as cloud cover, image acquisition time, and vegetation phenology variations. In the case of North Korea [5,22], land cover maps can classify broad categories, such as built-up land, forestland, farmland, and open water. However, more detailed and specific land classifications, such as sloping farmland and unstocked forestland, require higher-

resolution or multitemporal images as well as supportive in situ data for validation to determine the types of deforestation or degradation.

Since 2001, North Korea has attempted to restore forests with continuous reforestation plans; however, the restoration efforts have been inefficient [26]. Understanding the spatial and temporal changes in deforestation is a key requirement for managing ecosystem services and forest restoration [10,27]. The objectives of this study are to (1) propose a strategy for effectively extracting the two main types of forest cover loss, namely sloping farmland and unstocked forest, through the utilization of remote-sensing data; this strategy will provide a valuable tool for accurately quantifying and monitoring the extent of forest cover losses; (2) clarify the spatial and temporal distribution of the two types of forest cover loss; by analyzing these patterns, we can enable more targeted and informed conservation and management efforts; and (3) identify areas currently experiencing degradation as well as those at risk of degradation. By identifying these vulnerable regions, appropriate interventions and strategies can be developed and implemented to mitigate further forest cover loss and promote sustainable practices. In summary, the overarching purpose of this study is to provide insights and tools that contribute to the conservation and sustainable management of forest resources through accurate identification, understanding, and prevention of forest cover loss and degradation.

2. Materials and Methods

2.1. Study Area

North Korea is located in the north of the Korean Peninsula in East Asia, bordered by China and Russia to the north and South Korea to the south. North Korea covers an area of 123,354 km² (Figure 1). In total, 64% of the land area is sloping land with a slope greater than 6 degrees. Owing to the long-standing tectonic movements, erosion, and sedimentation, the topography is characterized by mountain areas, plains, valleys, coasts, and plateaus. Mountains with high elevations are concentrated in the north and east, whereas flat fields are mainly distributed on the west and south coasts. In North Korea, forestland and pasture areas have generally decreased and agricultural land, especially farmland on slopes, has increased in most areas. These changes are part of North Korea's policies, and the proportion of agricultural land is expected to increase until the 2030s.

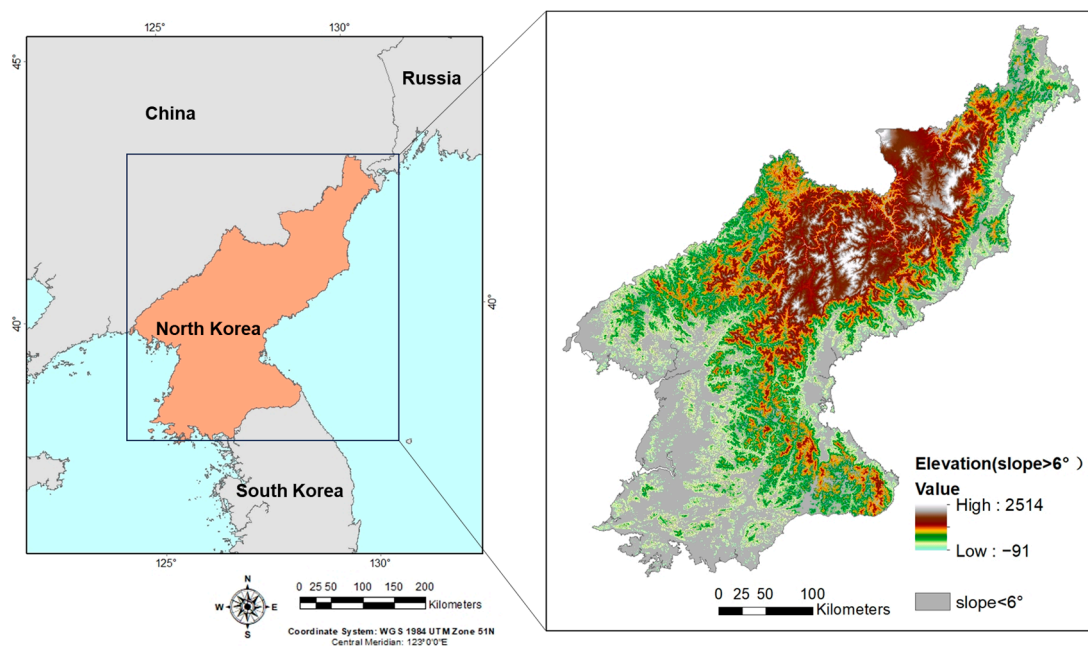


Figure 1. Study area. The elevation displayed is a 90 m resolution SRTM Digital Elevation Model.

Two main types of forest cover transitions are observed in North Korea: sloping farmland and unstocked forest. Sloping farmland is forestland with slopes greater than 6 degrees that was transformed into fields for cultivation. Once these sloping farmlands lose their productivity, they are left unmanaged and abandoned to form unstocked forest. Unstocked forest is a category of suitable forest land that has been cleared by logging or other causes and has not grown trees for a long time. Unstocked forest in North Korea usually occurs when sloping farmland is abandoned or after repeated artificial forest fires or logging. Therefore, the primary vegetation cover in forest land in North Korea is sloping farmland, unstocked forests, natural forests, and plateau areas.

2.2. Data Collection

2.2.1. Satellite Imagery

A reference forest cover map was required to identify sloping farmland and unstocked forests. Forests during the 1990s were selected as the reference and classified because the forests in North Korea exhibited a noticeable decreasing trend beginning in this period because of the local policy [28]. All images from the early 1990s with cloud cover less than 5% for 12 Landsat scene tiles covering North Korea were selected. All Landsat images were atmospherically corrected (Table 1). The scale was unified to 250 m to compare forest areas in the 1990s and other years.

Table 1. Information of remote-sensing data.

Years	Remote-Sensing Products	Tiles	Acquisition Date/Day of Year (DOY)
1990s	Landsat TM5 (30 m)	115/030; 115/031; 115/032; 115/033; 116/031; 116/032; 116/033; 116/034; 117/031; 117/032; 117/033; 118/032	3 July 1994; 3 July 1994; 3 July 1994; 12 August 1991; 28 May 1993; 20 May 1993; 2 June 1992; 2 June 1992; 27 May 1993; 27 May 1993; 1 June 1992; 15 September 1990
2000 2010 2015 2020	MOD13Q1 (250 m) NDVI, NIR, MIR band	H27V04; H27V05; H28V05	DOY 065~305

Since a single image can only provide limited information, it may fail to capture the complete complexity and variability of vegetation types. Moreover, Landsat images are affected by cloud cover, limiting the availability of cloud-free images for certain regions or periods. The coverage of North Korea provides limited image data with cloud cover below 5%. Additionally, these data are predominantly available during late autumn or winter, rendering it impossible to extract pertinent vegetation information.

To obtain the phenological characteristics of each type of vegetation, we used the Moderate Resolution Imaging Spectroradiometer (MODIS) MOD13Q1 product acquired from the USGS Earth Explorer. We used the Normalized Difference Vegetation Index (NDVI), band2 (NIR band), and band 7 (MIR band) from the product, which are related to plant growth and soil water, to distinguish the unique growth cycle. Considering the growth cycles of vegetation in North Korea, we used the product from March to October in 2000, 2010, and 2020 (Table 1).

2.2.2. Reference Data

Reference point data for each land cover class were collected based on field surveys and Google Earth. Due to the political isolation of North Korea, the survey points were collected only from the Chinese side of the Tumen River. We collected 112 GPS points from two deforestation landscapes in 2015 and simultaneously observed the deforestation pattern on the North Korean side of the river (Figure 1). We can interpret the visual criteria of the two deforestation patterns, which are difficult to distinguish in satellite images, through Google Earth. For the remaining land cover types, such as forest, built-up areas, farmland

(paddy), and water bodies, we applied the visual criteria interpreted in Jin et al. [6]. We ensured that a minimum of 200 samples were collected for each land cover type.

The points for testing classification accuracy were randomly created using ArcGIS 10.7 at each time point (2000, 2010, and 2020). Each class creates a minimum of 50 points with intervals over 500 m, and the points are overlaid on Google Earth to identify the land cover classes at every time point, by the same standards. For an objective evaluation, the survey team collected 115 points for two deforestation landscapes along the Tumen River in 2020 (Figure 2).

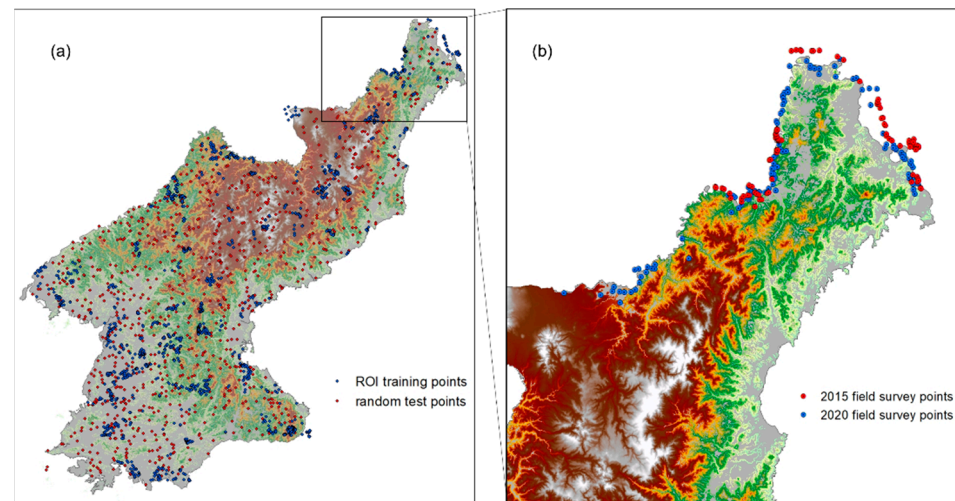


Figure 2. The region of interest (ROI) training and random test points (a) for model training, and field survey points along the Tumen River collected in 2015 and 2020 (b).

2.3. Land Cover Classification

Forests during the 1990s were used as reference forest maps. However, because of the limitations in satellite images, the classification of each land cover and deforested type was unclear. Thus, we only classified two types of land cover in the 1990s: forests and non-forests.

For 2000, 2010, and 2020 land cover maps, we classified six types of land cover in each study year: forest, unstocked forest, sloping farmland, farmland, water, and built-up areas (plateau area was added to the forest in the post-classification). Because of the similarity in the reflectance of each vegetation cover, the phenology-based indices derived from MODIS products were used to identify complex heterogeneous vegetation cover (Figure 3).

2.3.1. Normalized Indices

The transformation of spectral data into normalized indices greatly improved the classification accuracy. The Normalized Difference Vegetation Index (NDVI), an indicator of land degradation and increases or decreases in photosynthesis, was used as a predictor variable to capture the differences in land cover with optical sensors, thereby providing biophysical information.

However, the curves of vegetation cover types (forestland, plateau area, sloping farmland, and unstocked forest) followed the same general form. Therefore, a single index cannot effectively classify deforestation based on several vegetation cover types because similar values are obtained at a given time point [29,30].

Sloping farmland had the highest soil dryness compared to the forest landscapes. This was particularly evident when farmers prepared the fields early in the season, resulting in maximum soil exposure. From March to May, which marks the beginning of the growing season, the amount of soil exposed in the four different vegetation cover types varied

based on the presence of canopy. Thus, the Normalized Difference Water Index (NDWI, Equation (1)) [31] was selected to capture the difference in soil moisture.

$$\text{NDWI} = \frac{b_7 - b_2}{b_7 + b_2} \quad (1)$$

where b_2 and b_7 are the near-infrared band 2 and shortwave infrared band 7 of MODIS data, respectively. In this study, we calculated the NDVI and NDWI from March to October for the input variables without knowing in which month the difference occurred.

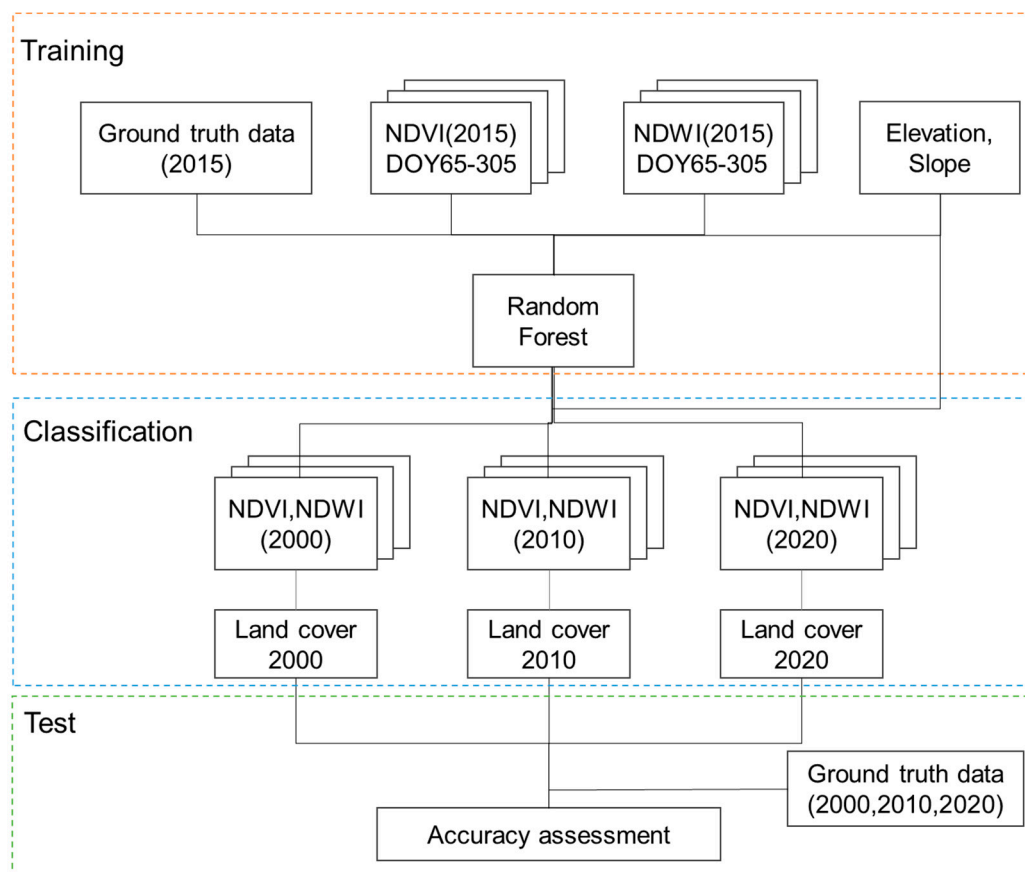


Figure 3. Flow of classification. The sample survey of the research area was conducted in 2015 and 2020. In situ data in 2015 and 2020 were used for training and testing the classification results for 2020.

2.3.2. Random Forest Classification

In addition to phenological indices, we utilized topography data, as well as elevation and slope, as predictor variables. We used a Random Forest (RF) classifier for deforestation classification. RF is an ensemble machine-learning method that integrates many decision trees into a forest and is used to train and classify sample data. One of the advantages of RF is that it can accurately predict the effects of up to thousands of explanatory variables and has been applied in remote-sensing classification studies [32]. When classifying data, the importance of each variable can also be scored and the role of each variable in the classification evaluated.

The RF model was built using the programming language R and implemented with the “randomForest” package [33]. Through previous experiments, ntree (the number of trees) was set to 500 and 100 runs. The accuracy of the trees was estimated using the out-of-bag prediction, which provides an unbiased estimate of map accuracy if the reference data were obtained through probability sampling. Finally, we estimated the overall accuracy, user’s

accuracy, producer's accuracy, and kappa coefficient through a confusion matrix to verify the results.

2.4. Spatiotemporal Analysis of Deforested Areas

To compare the forest losses in each time unit, we calculated the rate of deforestation. For the purpose of standardization and statistical comparability, we utilized the forest area data and time to determine a standardized deforestation rate based on the following formula [34]:

$$\text{rate} = \frac{1}{(t_2 - t_1)} \times \text{Ln} \left(\frac{A_2}{A_1} \right) \times 100 \quad (2)$$

where A_1 and A_2 are the deforested areas in years t_1 and t_2 , respectively. For example, for the period from $t_1 = 1990$ to $t_2 = 2000$, A_1 and A_2 are the values of deforested areas during 1990 and 2000, respectively.

Considering the reasons for the occurrence of unstocked forest and sloping farmland in North Korea, we can summarize four cases within the forestland of 1990 (Table 2). Forested land that was deforested and converted to unstocked forest in 2020, which was based on the unstocked periods, can be divided into two different cases: risk of degradation and degradation. Forest degradation is a long-term reduction in canopy cover and forest carbon stocks within the forest [35]. Thus, forestland under the unstocked status for an extended period can be regarded as forest degradation due to the low canopy cover and stocks. The forestland once used for crop production and converted into unstocked forest from 2010 to 2020 is regarded as at risk of degradation, and the area can be degraded if there is no management.

Table 2. Four cases of forestland changes from the 1990s to 2020 (F: forest; SF: sloping forest; UF: unstocked forest).

Cases	1990s	2000	2010	2020	Description
Case 1	F	F	SF/UF	F	Restoration, once deforested and restored
	F	SF/UF	F/SF/UF	F	
Case 2	F	F	F	SF/UF	Deforested land that in use
	F	F	SF/UF	SF	
	F	SF/UF	F/SF/UF	SF	
Case 3	F	F/SF	SF	UF	Risk of degradation, once deforested and abandoned.
	F	SF/UF	F	UF	
	F	SF/UF	SF	UF	
Case 4	F	F	UF	UF	Degradation, forestland converted to unstocked forest for a long time (over 2 decades)
	F	UF	UF	UF	
	F	SF	UF	UF	

3. Results

3.1. Accuracy Assessment of Classification

According to a UNEP report [36], the forest cover in 1990 was 82,000 km² (68% of the total land area), and our results for forestland in 1990s were 68.6%. From this, we can see that the UNEP data and our results for forested areas are nearly identical. The overall accuracy for 2000, 2010, and 2020 ranged from 87.1% to 88.6%, with kappa values from 0.84 to 0.86 (Figure 4). The results show that phenological indices can be used to distinguish similar spectral signatures, such as sloping farmland, unstocked forest, and other vegetation cover.

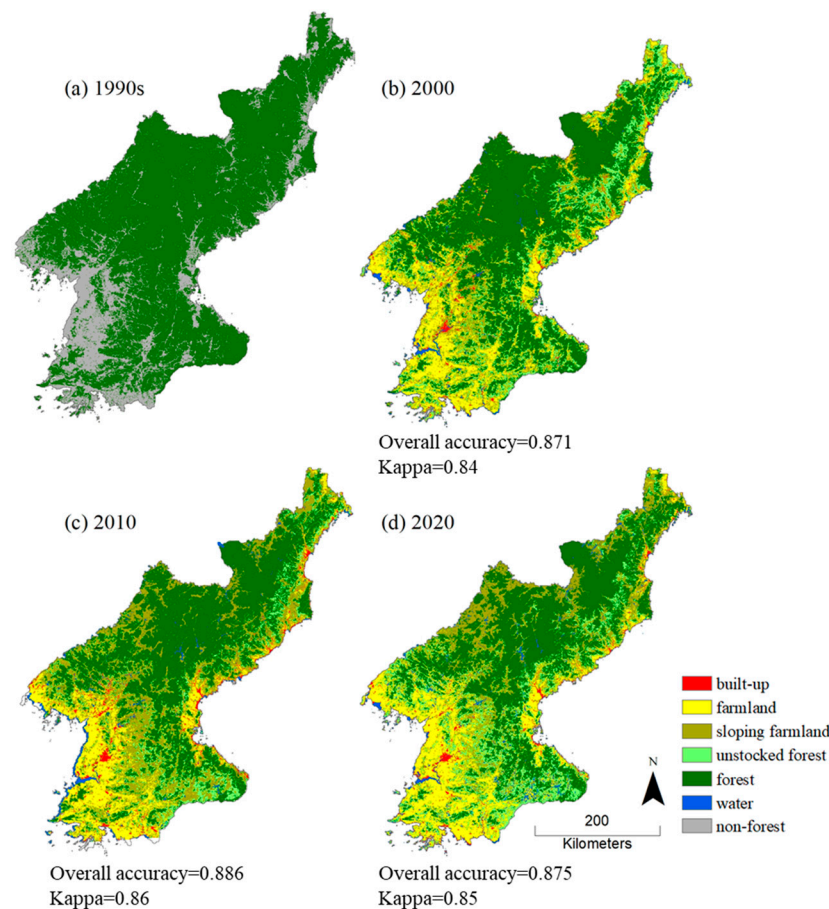


Figure 4. Results of the classification. Forest cover maps of the 1990s (a), and land cover maps for 2000 (b), 2010 (c), and 2020 (d).

The producer's accuracy and user's accuracy in mapping the built-up area, farmland, forest and water are higher than the sloping farmland and unstocked forest (Table 3, Appendix A). The classification accuracy of sloping farmland and unstocked forest is relatively lower compared to other types. The user's accuracy for sloping farmland is $89.8\% \pm 3.2\%$, with a producer's accuracy of $85.3\% \pm 5.4\%$. For unstocked forest, the user's accuracy is $86.5\% \pm 6.1\%$ and the producer's accuracy is $79\% \pm 3\%$. This is because similar spectral signatures in the vegetation cover types, sloping farmland are often misclassified as other categories, such as flat farmland or unstocked forests.

Table 3. Producer's and user's accuracy of land cover for land cover classification in the years 2000, 2010, and 2020.

Land Cover	User's Accuracy	Producer's Accuracy
Built-up	$98.5\% \pm 1.5\%$	$84.7\% \pm 4.9\%$
Farmland (flat land)	$84.6\% \pm 2.9\%$	$95\% \pm 3\%$
Sloping farmland	$89.8\% \pm 3.2\%$	$85.3\% \pm 5.4\%$
Unstocked forest	$86.5\% \pm 6.1\%$	$79\% \pm 3\%$
Forest	$81.6\% \pm 0.6\%$	$94.9\% \pm 0.8\%$
Water	$92.4\% \pm 3.5\%$	$95\% \pm 1\%$

3.2. Spatiotemporal Changes in Forest Cover

The extent of forest and deforestation from the 1990s to 2020 is shown in Figure 5. The forest cover that remained in 2020 accounted for 41.5% of the total land area, and the extent of forest cover decreased by nearly 27% over the 30-year study period. As summarized in

Table 4, the loss of forest cover in the 1990s was much greater than that from 2000 to 2010 or 2010 to 2020. The rate of forest loss was 1.7% per year on average throughout the study period. The first decade of analysis (1990s–2000) contributed 67.3% of total forest loss, the rate of forest loss in this period was 3.1% per year and most forest cover was converted to sloping farmland and unstocked forest. The second decade (2000–2010) and third decade (2010–2020) accounted for 14.8% and 17.9% of forest loss, respectively, and these values were less than half the rate in the 1990s.

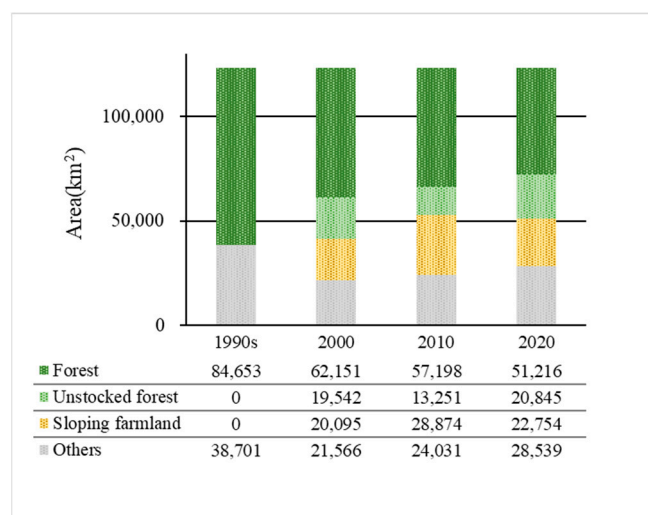


Figure 5. Changes in vegetation cover types in North Korea from the 1990s to 2020. The total area of North Korea is 123,354 km².

Table 4. Changes in forest cover area and rate from the 1990s to 2020.

	1990s–2000	2000–2010	2010–2020	1990s–2020
Forest loss (rate)	24,302 (−3.1%)	4953 (−0.8%)	5982 (−1.1%)	33,437 (−1.7%)
Forest to sloping farmland	8777	5961	5125	14,184
Forest to unstocked forest	15,992	6484	7156	17,657
Forest to others	3946	348	356	4249
Restoration	4413	7840	6555	
Case 1: Restoration				8940
Case 2: Deforestation				18,263
Case 3: Risk of degradation				6728
Case 4: Degradation				5346

As the forest near the village is damaged owing to the expansion of farmland, it can be estimated that deforestation is proceeding in the core area and causing severe fragmentation. The decrease in forestland and fragmentation can affect ecological connectivity and biodiversity. For example, the forest in North Korea is in an important position to link ecological networks from Mt. Changbai (the border of China and North Korea) to Mt. Jiri (South Korea). However, deforestation causes forests to gradually shrink, especially on the North Korean–South Korean and North Korean–Chinese borders, and substantial fragmentation has been observed in these areas (Figures 6 and 7).

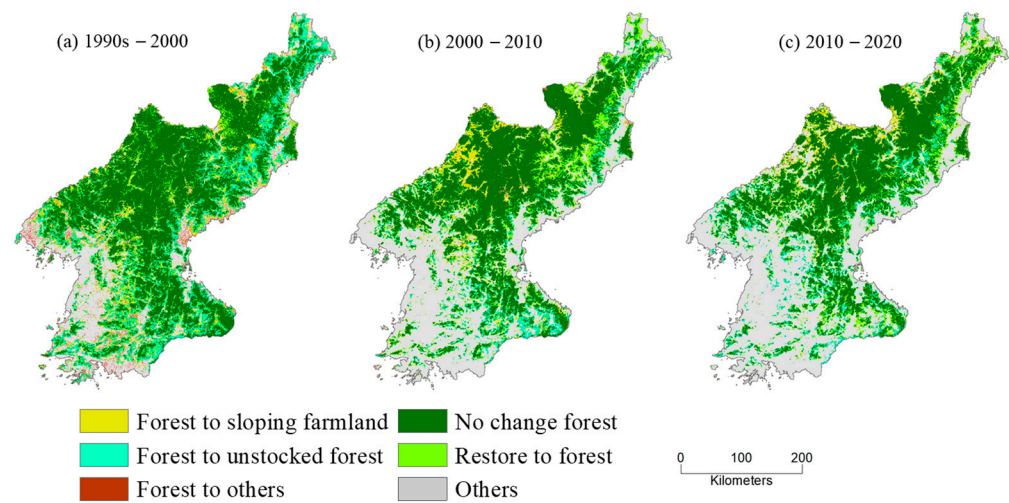


Figure 6. Deforestation occurred from 1990 to 2000 (a); from 2000 to 2010 (b), and from 2010 to 2020 (c).

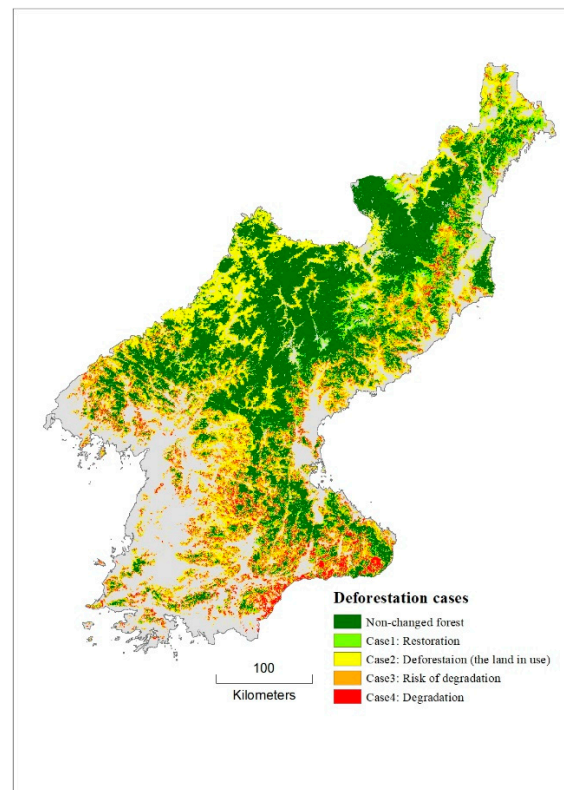


Figure 7. Deforestation cases in North Korea from 1990s to 2020.

Among the forestland utilization types, the highest rates of forest loss were observed for unstocked forest and sloping farmland, which accounted for 48.9% and 39.3% of the total loss during the study period, respectively. From the 1990s to 2000, North Korea experienced extensive deforestation. The area of newly increased unstocked forest and sloping farmland accounted for 86% of the total forest loss, and the unstocked forest area was nearly twice that of the sloping farmland area. Since 2000, deforestation has decreased significantly, newly increased sloping farmland and unstocked forest have also declined, and restoration of sites to forest has increased (Figure 6). The greening policies in North Korea, which began in 2001, slowed the rate of deforestation and improved forest restoration.

Although the rate of deforestation has decreased and nationwide restoration efforts are ongoing, deforested areas have increased during each period of study. Moreover, the

low efficiency of restoration cannot keep up with the rate of deforestation. Due to the different land use change histories, the soil status and abandonment period are different, which necessitate appropriate measurements. Most of the forestland deforested in the 1990s was turned into sloping farmland (14,184 km²) and unstocked forest (17,657 km²) by 2020, between which interchangeable uses were observed. Most of the sloping farmland had been used for a long time (case two, 18,623 km²) and was eventually abandoned without management (case three, 6728 km²). Moreover, owing to repeated fires, some unstocked forests have long had an unstocked land status and have degraded (case four, 5324 km²) (Table 4).

Large areas of degradation and land at risk of degradation are connected with sloping farmland distributed along the edge of forestlands, resulting in shrinking and fragmentation (Figure 7). The denuded slopes are desolate and can be observed on the Chinese side of the Tumen River and along the border between North Korea and South Korea in the summer. Because of the political tension between North and South Korea, most of these desolate areas are caused by fires at the borders. Abandoned slopes mainly generate areas with low productivity that are not managed. These areas are unsustainable and have poor ecological functions, and they have become increasingly degraded until reaching an unstocked status [26].

4. Discussion

The two deforestation patterns in North Korea, namely, sloping farmland and unstocked forest, reduce the ability to withstand natural disasters. Large-scale forest fires, commercial logging, and expanding farmlands in hilly areas are the main drivers of deforestation and forest degradation in North Korea. Our results provide a comprehensive deforestation map of the two classes of deforested land. Between 1990 and 2020, forestland areas of 14,181 km² and 17,657 km² were converted to sloping farmland and unstocked forest, respectively, and these trends are consistent with other research on North Korea [5]. In addition, this study presents a spatiotemporal trajectory analysis for the first time for the detection of two patterns of deforestation in North Korea.

To validate the estimated forest cover transitions, we conducted a comparison with the GLAD Global Land Cover and Land Use Changes dataset [37]. This dataset measures changes in forest extent from the year 2000 to 2020 at a spatial resolution of 30 m. Our findings indicate that 41.5% of the total land area remained unchanged as forest from 2000 to 2020, whereas the GLAD dataset shows a stable forest area of 49.5%. The variation in these numbers can be attributed to discrepancies in spatial resolution. A limitation of our study was the use of a 250 m pixel resolution, which presented challenges in classifying fragmented forest areas. The comparison of forest cover distribution demonstrates that our results align well with the spatial distribution of forest core areas and forest disturbances in the GLAD dataset (Figure 8). In contrast, our findings reveal that 13.6% of the forested land underwent conversion into sloping farmland or unstocked forest, whereas the GLAD dataset indicates a much lower transformation rate of 3.74% into short vegetation and cropland.

Therefore, we compared it with Google Earth imagery (Figure 9). The analysis of Figure 9 reveals that the pointed area in the 2018 image represents extensive sloping farmland. However, the GLAD dataset classifies it as short vegetation, which aligns with our study's characterization of unstocked forest cover. This discrepancy may arise due to the GLAD dataset's focus on global land use, which might not fully account for the distinct land use characteristics of individual countries. Our research excels in its comprehensive examination of North Korea's land use characteristics, enabling us to analyze the dynamic patterns of forest cover transition.

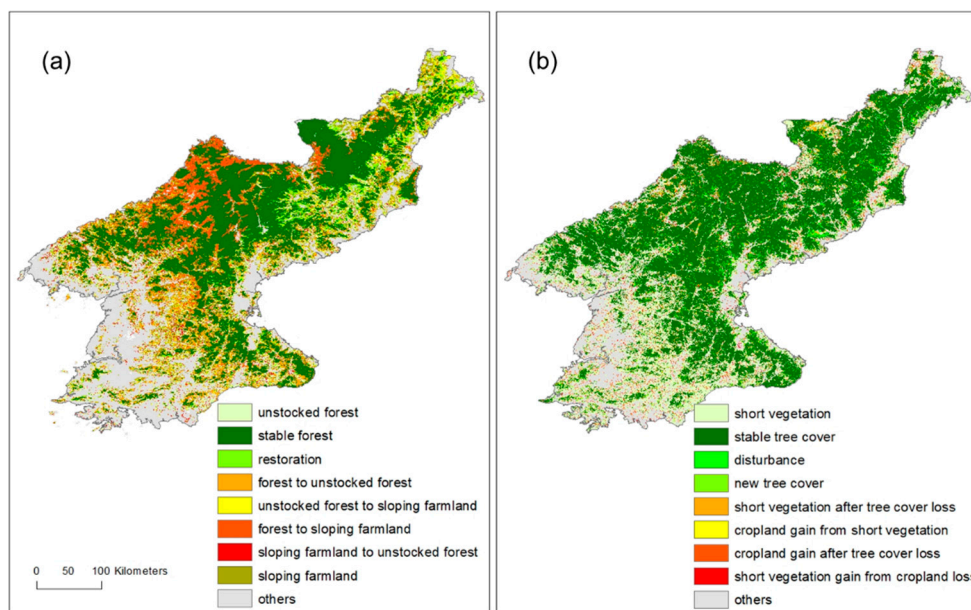


Figure 8. Comparison of our results on forest cover changes occurred from 2000 to 2020 (a) with the GLAD dataset (b).

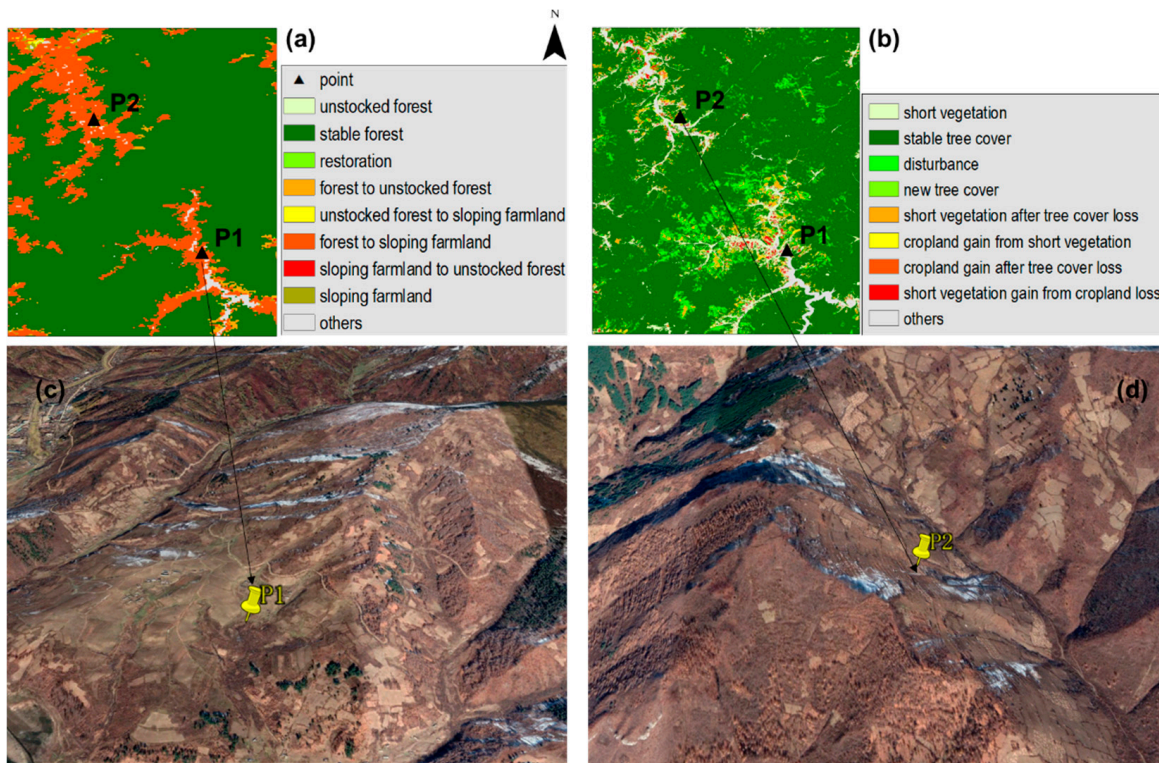


Figure 9. Comparison of our results (a) with the GLAD dataset (b) and a Google Earth Image taken on 2 November 2018 (c,d). The geographical coordinates of the points are P1: 40°57'7.29" N, 127°8'49.28" E; P2: 41°10'45.41" N, 126°57'31.03" E.

Many studies have attempted to quantify North Korea’s scale of deforestation, with many indicating that deforestation is a result of forest conversion to cropland; however, the discussion on unstocked forests is insufficient. Unstocked woods, which are temporarily devoid of forest growth, are among the main manifestations of deforestation in North Korea. Long periods of abandonment, low production, logging, and forest fires can all cause

unstocked forests. Therefore, it is impossible to determine whether an area is degraded by analyzing the unstocked forest at only one time point. A forest with a long unstocked period can be regarded as an unproductive area in the process of degradation [38]. Through the analysis of the past 30 years of deforestation, we can identify forestland that is in the process of degradation and land that is at risk of degradation.

To perform effective forest rehabilitation, it is necessary to consider forestland dynamics reflected in differentiated reforestation planning. The Korean Peninsula experienced a similar conversion of forestland in North and South Korea. South Korea has succeeded in restoring the forest ecosystem, whereas North Korea has not successfully restored its forests, even with continuous reforestation planning. The difference between the two countries is the financial situation and rehabilitation projects.

Different reforestation planning strategies have been applied in South Korea based on the forestland status. To restore degraded land and prevent soil erosion, fast-growing tree species have been planted in areas that have been deforested. Additionally, the practice of slash-and-burn farming has been eliminated, which has contributed to the successful restoration of forests. To establish effective forest management, the economic functions and public benefits of forests have also been considered. Through the successful reforestation of South Korea [26], we can see that different strategies have been implemented for different statuses of forestland. Therefore, deforested landscapes must be classified to perform reforestation planning.

We proposed a new set of maps to quantify the extent of deforestation and degradation and the risk of degradation in North Korea and used observation reference data and phenology-based indices for 2015 to predict land cover in 2000, 2010, and 2020. Although this approach consistently increased individual classification accuracy, the above quantification still contained some errors. Because a slight gap in phenology occurred between the survey year and prediction year, which can affect the results, this study used the monthly average of indices to reduce the uncertainty generated by the temporal interval. To improve the accuracy of deforestation mapping, it is necessary to observe the phenology of each vegetation cover type. Furthermore, the phenology of the target year differed from that of the year in which the model was constructed. In such cases, the classification model should be reconstructed and indices that have the greatest impact on the target year should be identified. The classification method proposed in this study for mapping deforestation will be valuable for monitoring areas with diverse vegetation cover in mountainous regions. Moreover, this approach can also be utilized in situations where accessing field data is difficult and there is a lack of historical information. It enables us to better understand and manage forest resources, ultimately contributing to a more sustainable and resilient ecosystem. However, further research and field surveys are necessary to enhance the techniques for classifying different types of vegetative cover at high spatial resolutions.

5. Conclusions

The three decades from 1990 to 2020 witnessed an increase in deforestation of sloping farmland and unstocked forest. Almost 39.4% of the remaining forestland in 1990 was lost by 2020. The rate of forest loss reached 3.1% per year before 2000 and began to decline after 2000 because of forest policies; however, forest loss continues. The most severe deforestation occurred from 1990 to 2000, and 13.68% of the deforested land continued to be used as sloping farmland by 2020. Deforestation spread into the core area and caused severe shrinking and fragmentation, while the edge of the forestland was degraded or at risk of degradation. Although reforestation policies can decrease the rate of forest loss, the effectiveness of reforestation requires both technological and cooperative management.

North Korea is a region where forest conservation and development demands exist. Therefore, there is an urgent need for preservation and sustainable development. For effective management and reforestation, in-depth research should be conducted, such as investigations of site-specific characteristics, surveys of forest ecological functions, and the selection of priority restoration areas. This study provides insights that are useful for

planning reforestation projects, reaching conservation targets, and improving ecosystem services for the entire Korean Peninsula.

Author Contributions: Conceptualization, Y.J. and D.K.L.; Data curation, Y.J.; Formal analysis, Y.J.; Funding acquisition, G.C. and Z.Y.; Investigation, Y.J., J.Z. and Z.Y.; Methodology, Y.J., J.Z. and G.C.; Project administration, Y.J.; Supervision, Y.J.; Validation, Z.Y. and W.Z.; Visualization, Y.J.; Writing—original draft, Y.J.; Writing—review and editing, Y.J. All authors have read and agreed to the published version of the manuscript.

Funding: This research was funded by the National Natural Science Foundation of China (grant number 42061042 and 41977401), and Natural Science Foundation of Jilin Province of China (NO. 20200201044JC).

Data Availability Statement: The data that support the findings of this study are available on request from the first author and corresponding author.

Conflicts of Interest: The authors declare no conflict of interest.

Appendix A

Table A1. The confusion matrix for the land cover classification of 2000.

	Built Up	Farmland	Sloping Farmland	Unstocked Forest	Forest	Water	Total	User's Accuracy
Built up	72	6	0	0	0	12	90	0.8
Farmland	0	98	2	0	0	0	100	0.98
Sloping farmland	0	6	78	0	2	0	86	0.907
Unstocked forest	0	0	6	76	18	0	100	0.76
Forest	0	0	0	6	92	0	98	0.939
Water	2	2	0	0	0	96	100	0.96
Total	74	112	86	82	112	108	574	
Producer's Accuracy	0.973	0.875	0.927	0.927	0.821	0.889		

Table A2. The confusion matrix for the land cover classification of 2010.

	Built Up	Farmland	Sloping Farmland	Unstocked Forest	Forest	Water	Total	User's Accuracy
Built up	86	4	0	0	2	4	96	0.896
Farmland	0	92	2	6	0	0	100	0.92
Sloping farmland	0	6	80	8	6	0	100	0.8
Unstocked forest	0	0	4	82	14	0	100	0.82
Forest	0	0	0	6	94	0	100	0.94
Water	0	6	0	0	0	94	100	0.94
Total	86	108	86	102	116	98	596	
Producer's Accuracy	1	0.852	0.93	0.804	0.81	0.959		

Table A3. The confusion matrix for the land cover classification of 2020.

	Built Up	Farmland	Sloping Farmland	Unstocked Forest	Forest	Water	Total	User's Accuracy
Built up	82	10	2	0	2	4	100	0.82
Farmland	0	98	0	2	0	0	100	0.98
Sloping farmland	0	8	78	4	6	0	96	0.812
Unstocked forest	0	0	10	76	14	0	100	0.76
Forest	0	0	0	4	96	0	100	0.96
Water	0	4	0	0	0	90	94	0.957
Total	82	120	90	86	118	94	590	
Producer's Accuracy	1	0.817	0.867	0.883	0.814	0.957		

References

- Finer, M.; Novoa, S.; Weisse, M.J.; Petersen, R.; Mascaro, J.; Souto, T.; Stearns, F.; Martinez, R.G. Combating deforestation: From satellite to intervention. *Science* **2018**, *360*, 1303–1305. [[CrossRef](#)] [[PubMed](#)]
- Xiong, B.; Chen, R.; Xia, Z.; Ye, C.; Anker, Y. Large-scale deforestation of mountainous areas during the 21st Century in Zhejiang Province. *Land Degrad. Dev.* **2020**, *31*, 1761–1774. [[CrossRef](#)]
- Araza, A.B.; Castillo, G.B.; Buduan, E.D.; Hein, L.; Herold, M.; Reiche, J.; Gou, Y.; Villaluz, M.G.Q.; Razal, R.A. Intra-Annual Identification of Local Deforestation Hotspots in the Philippines Using Earth Observation Products. *Forests* **2021**, *12*, 1008. [[CrossRef](#)]
- Pfaff, A.; Amacher, G.S.; Sills, E.O.; Coren, M.J.; Streck, C.; Lawlor, K. Deforestation and Forest Degradation: Concerns, Causes, Policies, and Their Impacts. In *Encyclopedia of Energy, Natural Resource, and Environmental Economics*; Shogren, J.F., Ed.; Elsevier: Waltham, MA, USA, 2013; pp. 144–149.
- Lim, C.-H.; Song, C.; Choi, Y.; Jeon, S.W.; Lee, W.-K. Decoupling of forest water supply and agricultural water demand attributable to deforestation in North Korea. *J. Environ. Manag.* **2019**, *248*, 109256. [[CrossRef](#)]
- Jin, Y.; Sung, S.; Lee, D.K.; Biging, G.S.; Jeong, S. Mapping Deforestation in North Korea Using Phenology-Based Multi-Index and Random Forest. *Remote Sens.* **2016**, *8*, 997. [[CrossRef](#)]
- Engler, R.; Teplyakov, V.; Adams, J.M. An assessment of forest cover trends in South and North Korea, from 1980 to 2010. *Environ. Manag.* **2014**, *53*, 194–201. [[CrossRef](#)]
- Kim, G.S.; Lim, C.-H.; Kim, S.J.; Lee, J.; Son, Y.; Lee, W.-K. Effect of National-Scale Afforestation on Forest Water Supply and Soil Loss in South Korea, 1971–2010. *Sustainability* **2017**, *9*, 1017. [[CrossRef](#)]
- Lee, J.; Lim, C.-H.; Kim, G.S.; Markandya, A.; Chowdhury, S.; Kim, S.J.; Lee, W.-K.; Son, Y. Economic viability of the national-scale forestation program: The case of success in the Republic of Korea. *Ecosyst. Serv.* **2018**, *29*, 40–46. [[CrossRef](#)]
- Bagan, H.; Millington, A.; Takeuchi, W.; Yamagata, Y. Spatiotemporal analysis of deforestation in the Chapare region of Bolivia using LANDSAT images. *Land Degrad. Dev.* **2020**, *31*, 3024–3039. [[CrossRef](#)]
- Seymour, F.; Harris, N.L. Reducing tropical deforestation. *Science* **2019**, *365*, 756–757. [[CrossRef](#)]
- Soto Vega, P.J.; Costa, G.A.O.P.d.; Feitosa, R.Q.; Ortega Adarme, M.X.; Almeida, C.A.d.; Heipke, C.; Rottensteiner, F. An unsupervised domain adaptation approach for change detection and its application to deforestation mapping in tropical biomes. *ISPRS J. Photogramm. Remote Sens.* **2021**, *181*, 113–128. [[CrossRef](#)]
- Spröhnle, K.; Kranz, O.; Schoepfer, E.; Moeller, M.; Voigt, S. Earth observation-based multi-scale impact assessment of internally displaced person (IDP) camps on wood resources in Zalingei, Darfur. *Geocarto Int.* **2016**, *31*, 575–595. [[CrossRef](#)]
- Sboui, T.; Saidi, S.; Lakti, A. A Machine-Learning-Based Approach to Predict Deforestation Related to Oil Palm: Conceptual Framework and Experimental Evaluation. *Appl. Sci.* **2023**, *13*, 1772. [[CrossRef](#)]
- Dominguez, D.; del Villar, L.d.J.; Pantoja, O.; González-Rodríguez, M. Forecasting Amazon Rain-Forest Deforestation Using a Hybrid Machine Learning Model. *Sustainability* **2022**, *14*, 691. [[CrossRef](#)]
- Solórzano, J.V.; Mas, J.F.; Gallardo-Cruz, J.A.; Gao, Y.; Fernández-Montes de Oca, A. Deforestation detection using a spatio-temporal deep learning approach with synthetic aperture radar and multispectral images. *ISPRS J. Photogramm. Remote Sens.* **2023**, *199*, 87–101. [[CrossRef](#)]
- Tarazona, Y.; Zabala, A.; Pons, X.; Broquetas, A.; Nowosad, J.; Zurqani, H.A. Fusing Landsat and SAR Data for Mapping Tropical Deforestation through Machine Learning Classification and the PVts- β Non-Seasonal Detection Approach. *Can. J. Remote Sens.* **2021**, *47*, 677–696. [[CrossRef](#)]
- Liu, Y.; Zhang, R.; Lin, C.-F.; Zhang, Z.; Zhang, R.; Shang, K.; Zhao, M.; Huang, J.; Wang, X.; Li, Y.; et al. Remote sensing of subtropical tree diversity: The underappreciated roles of the practical definition of forest canopy and phenological variation. *For. Ecosyst.* **2023**, *10*, 100122. [[CrossRef](#)]
- Herraiz, A.D.; Salazar-Zarzosa, P.C.; Mesas, F.J.; Arenas-Castro, S.; Ruiz-Benito, P.; Villar, R. Modelling aboveground biomass and productivity and the impact of climate change in Mediterranean forests of South Spain. *Agric. For. Meteorol.* **2023**, *337*, 109498. [[CrossRef](#)]
- Ponte, E.D.; Molas, L.P.d.; García-Calabrese, M.; Kriese, J.; Cabral, N.; Alvarenga, M.; Caceres, A.; Gali, A.; García, V.; Morinigo, L.; et al. Understanding 34 Years of Forest Cover Dynamics across the Paraguayan Chaco: Characterizing Annual Changes and Forest Fragmentation Levels between 1987 and 2020. *Forests* **2022**, *13*, 25. [[CrossRef](#)]
- Piao, Y.; Xiao, Y.; Ma, F.; Park, S.; Lee, D.; Mo, Y.; Jeong, S.; Hwang, I.; Kim, Y. Monitoring Land Use/Land Cover and Landscape Pattern Changes at a Local Scale: A Case Study of Pyongyang, North Korea. *Remote Sens.* **2023**, *15*, 1592. [[CrossRef](#)]
- Piao, Y.; Jeong, S.; Park, S.; Lee, D. Analysis of Land Use and Land Cover Change Using Time-Series Data and Random Forest in North Korea. *Remote Sens.* **2021**, *13*, 3501. [[CrossRef](#)]
- Kang, S.; Choi, J.; Yoon, H.; Choi, W. Changes in the extent and distribution of urban land cover in the Democratic People's Republic of Korea (North Korea) between 1987 and 2010. *Land Degrad. Dev.* **2019**, *30*, 2009–2017. [[CrossRef](#)]
- Kang, S.; Choi, W. Forest cover changes in North Korea since the 1980s. *Reg. Environ. Change* **2014**, *14*, 347–354. [[CrossRef](#)]
- Lim, C.-H.; Choi, Y.; Kim, M.; Jeon, S.; Lee, W.-K. Impact of Deforestation on Agro-Environmental Variables in Cropland, North Korea. *Sustainability* **2017**, *9*, 1354. [[CrossRef](#)]
- Park, M.; Lee, H. Forest Policy and Law for Sustainability within the Korean Peninsula. *Sustainability* **2014**, *6*, 5162–5186. [[CrossRef](#)]

27. Bovolo, C.I.; Donoghue, D.N.M. Has regional forest loss been underestimated? *Environ. Res. Lett.* **2017**, *12*, 111003. [[CrossRef](#)]
28. Schwekendiek, D. Regional variations in living conditions during the North Korean food crisis of the 1990s. *Asia Pac. J. Public Health* **2010**, *22*, 460–476. [[CrossRef](#)]
29. Zhong, L.; Hu, L.; Yu, L.; Gong, P.; Biging, G.S. Automated mapping of soybean and corn using phenology. *ISPRS J. Photogramm. Remote Sens.* **2016**, *119*, 151–164. [[CrossRef](#)]
30. Ashourloo, D.; Nematollahi, H.; Huete, A.; Aghighi, H.; Azadbakht, M.; Shahrabi, H.S.; Goodarzashti, S. A new phenology-based method for mapping wheat and barley using time-series of Sentinel-2 images. *Remote Sens. Environ.* **2022**, *280*, 113206. [[CrossRef](#)]
31. Gao, B.-C. NDWI—A normalized difference water index for remote sensing of vegetation liquid water from space. *Remote Sens. Environ.* **1996**, *58*, 257–266. [[CrossRef](#)]
32. Pal, M. Random forest classifier for remote sensing classification. *Int. J. Remote Sens.* **2005**, *26*, 217–222. [[CrossRef](#)]
33. Liaw, A.; Wiener, M. Classification and Regression by randomForest. *R News* **2002**, *2*, 18–22.
34. Jönsson, P.; Eklundh, L. TIMESAT—A program for analyzing time-series of satellite sensor data. *Comput. Geosci.* **2004**, *30*, 833–845. [[CrossRef](#)]
35. Schoene, D.; Killmann, W.; Lüpke, H.; LoycheWilkie, M. *Definitional Issues Related to Reducing Emissions from Deforestation in Developing Countries*; FAO: Rome, Italy, 2007.
36. Piddington, K. *DPR KOREA: State of the Environment Report*; UNEP: Pathumthani, Thailand, 2003.
37. Potapov, P.; Li, X.; Hernandez-Serna, A.; Tyukavina, A.; Hansen, M.C.; Kommareddy, A.; Pickens, A.; Turubanova, S.; Tang, H.; Silva, C.E.; et al. Mapping global forest canopy height through integration of GEDI and Landsat data. *Remote Sens. Environ.* **2021**, *253*, 112165. [[CrossRef](#)]
38. Han, Y.; Ke, Y.; Zhu, L.; Feng, H.; Zhang, Q.; Sun, Z.; Zhu, L. Tracking vegetation degradation and recovery in multiple mining areas in Beijing, China, based on time-series Landsat imagery. *GIScience Remote Sens.* **2021**, *58*, 1477–1496. [[CrossRef](#)]

Disclaimer/Publisher’s Note: The statements, opinions and data contained in all publications are solely those of the individual author(s) and contributor(s) and not of MDPI and/or the editor(s). MDPI and/or the editor(s) disclaim responsibility for any injury to people or property resulting from any ideas, methods, instructions or products referred to in the content.